Acta Crystallographica Section C
Crystal Structure Communications
ISSN 0108-2701

(1*H*-Pyrazole-κN^2)(2,2′:6′,2″-terpyridine-$\kappa^3 N,N',N''$)platinum(II) bis(perchlorate) nitromethane monosolvate

Matthew Akerman,* Kate Akerman, Deogratius Jaganyi and Desigan Reddy

School of Chemistry, University of KwaZulu-Natal, Private Bag X01, Pietermaritzburg 3209, South Africa
Correspondence e-mail: akermanm@ukzn.ac.za

Received 7 May 2011
Accepted 30 June 2011
Online 6 August 2011

The reaction between [PtCl(terpy)]·2H_2O (terpy is 2,2′:6′,2″-terpyridine) and pyrazole in the presence of two equivalents of $AgClO_4$ in nitromethane yields the title compound, $[Pt(C_3H_4N_2)(C_{15}H_{11}N_3)](ClO_4)_2{\cdot}CH_3NO_2$, as a yellow crystalline solid. Single-crystal X-ray diffraction shows that the dicationic platinum(II) chelate is square planar with the terpyridine ligand occupying three sites and the pyrazole ligand occupying the fourth. The torsion angle subtended by the pyrazole ring relative to the terpyridine chelate is 62.4 (6)°. Density functional theory calculations at the LANL2DZ/PBE1PBE level of theory show that *in vacuo* the lowest-energy conformation has the pyrazole ligand in an orientation perpendicular to the terpyridine ligand (*i.e.* 90°). Seemingly, the stability gained by the formation of hydrogen bonds between the pyrazole NH group and the perchlorate anion in the solid-state structure is sufficient for the chelate to adopt a higher-energy conformation.

Comment

Platinum(II) chelates have been extensively studied since their application as antitumour agents was discovered in the 1960s (Jaganyi *et al.*, 2008). Although *cis*-diamminedichloroplatinum(II) (cisplatin) has been effective in the treatment of particular tumour cell lines, cisplatin resistance in certain cancer cell lines has sparked much research into developing new-generation platinum-based drugs (Thurston, 2007). The substitution kinetics of the title metal chelate have been studied to further develop the understanding of the interactions between the Pt^{II} ion and various nucleophiles. This research is critical to the development of new drugs (Jaganyi *et al.*, 2008). The structure of the title pyrazole-substituted terpyridine–platinum(II) compound, $[Pt(pyz)(terpy)](ClO_4)_2{\cdot}CH_3NO_2$ (where terpy is 2,2′:6′,2″-terpyridine and pyz is pyrazole), (I), was elucidated to further develop the understanding of the binding mode of the ancillary ligand, *i.e.* whether the pyrazole ligand was deprotonated or not.

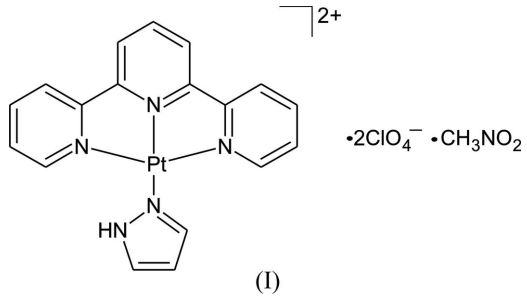

(I)

A search of the Cambridge Structural Database (CSD; *ConQuest* Version 1.12; Allen, 2002) showed that the title compound is a novel structure. There is, however, a reported μ_2-pyrazolyl structure (Bailey & Gray, 1992), where the reported metal chelate was synthesized under basic conditions and, as a result, the pyrazole ligand is deprotonated and a terpyridine–platinum(II) cation is bound to each N atom of the ancillary ligand. The pyrazolyl ligand thus bridges the two chelates.

The title metal chelate crystallized in the monoclinic space group $P2_1/c$ with $Z = 4$. The cation in the asymmetric unit is associated with two perchlorate anions and a nitromethane solvent molecule (see Fig. 1 and below). In the title compound, the pyrazole ligand has bound in a more conventional manner than the previously reported μ_2-pyrazolyl structure, with the nucleophilic ligand displacing the chloride ligand and covalently bonding to the metal centre. The pyrazole ligand occupies the fourth site of the Pt^{II} centre, while the terpyridine ligand occupies the other three binding sites, giving a square-planar metal chelate. The Pt1—N1, Pt1—N3 and Pt1—N4 bond lengths are approximately equal at 2.022 (6), 2.018 (6) and 2.011 (6) Å, respectively. The Pt1—N2 bond distance is

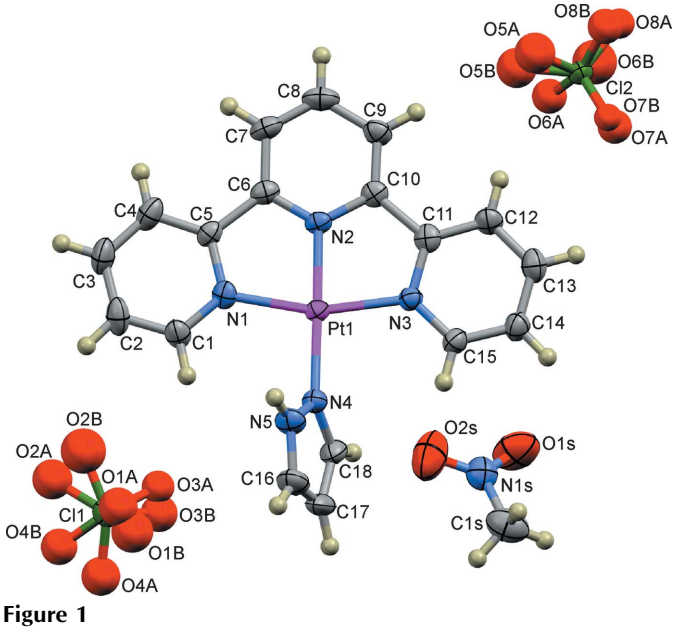

Figure 1
Displacement ellipsoid plot (30% probability level) of the title compound.

  doi:10.1107/S0108270111026011

noticeably shorter at 1.922 (6) Å (refer to Fig. 1 for the numbering scheme). The Pt^{II} ion is displaced from the least-squares plane defined by the four coordinating N atoms by 0.027 (1) Å. As expected, the N1—Pt1—N4 and N3—Pt1—N4 angles are approximately equal at 98.1 (3) and 99.3 (3)°, respectively. Similarly, the N1—Pt1—N2 and N2—Pt1—N3 angles are similar in magnitude at 80.9 (3) and 81.7 (3)°, respectively. These bond lengths and angles show no noteworthy deviation from those previously reported for similar platinum(II) chelates (Field *et al.*, 2007). It would appear that in the absence of a strong base the pyrazole ligand will preferentially bind through the N atom of the ancillary ligand as opposed to through the deprotonated NH atom.

Insofar as the packing of the metal cation is concerned, the metal chelate reported in this work is devoid of any Pt···Pt or π–π interactions as the chelates are not arranged parallel to one another. This is likely due to electrostatic repulsion between the highly charged chelates (dicationic as compared to monocationic species with this ligand architecture) (Field *et al.*, 2003). This repulsion overrides any attractive force from Pt···Pt or π–π interactions.

The structure exhibits a number of hydrogen bonds. The perchlorate anions are hydrogen bonded to both the nitromethane solvent in the lattice and the pyrazole NH group. In addition to this there are numerous aromatic–perchlorate C—H···O interactions. In all cases, the perchlorate O atoms act as hydrogen-bond acceptors and the pyrazole N—H and aromatic C—H groups act as donors. There are additional hydrogen bonds in the lattice between the aromatic C—H groups and the perchlorate anions; however, these interactions are longer than the sum of the van der Waals radii minus 0.1 Å and are therefore likely to be weak hydrogen bonds and are not discussed. Each methyl group of the nitromethane molecule bridges two perchlorate anions through hydrogen bonding. These perchlorate anions are in turn hydrogen bonded to two adjacent platinum(II) chelates. This combination of hydrogen bonds allows for the formation of an extended three-dimensional supramolecular structure. The hydrogen-bond lengths and angles are summarized in Table 1.

The hydrogen-bond lengths in Table 1 are all shorter than the sum of the van der Waals radii minus 0.1 Å. Although hydrogen-bond length does not necessarily correlate linearly with bond strength because of packing constraints in the lattice, it is probable that these bonds are moderate in strength as the bond lengths are considerably shorter than the van der Waals radii of the atoms. In addition to their short length, the bonds are reasonably linear, which can also indicate a moderately strong bond. The strongly electron-withdrawing nitro group of the solvent will result in a more polar C—H bond than usual and as such could increase the strength of this hydrogen bond, based on simple electrostatic arguments.

The pyrazole ligand is neither coplanar with nor perpendicular to the terpyridine ligand; the N1—Pt—N4—N5 torsion angle is 62.4 (6)°. The structure of the metal chelate *in vacuo* was calculated using density functional theory (DFT) methods at the PBE1PBE/LANL2DZ level of theory. PBE1PBE (Perdew *et al.*, 1997) is a gradient-corrected functional. The LANL2DZ (Hay & Dunning, 1976; Hay & Wadt, 1985*a*,*b*,*c*) basis set makes use of effective core potentials to deal with atoms in the second row of the periodic table and beyond. The DFT calculations were all performed with *GAUSSIAN03W* (Frisch *et al.*, 2004) with no symmetry constraints imposed on any of the calculations. The fractional coordinates from the structure determination were used as the starting point for a full geometry optimization of the cation.

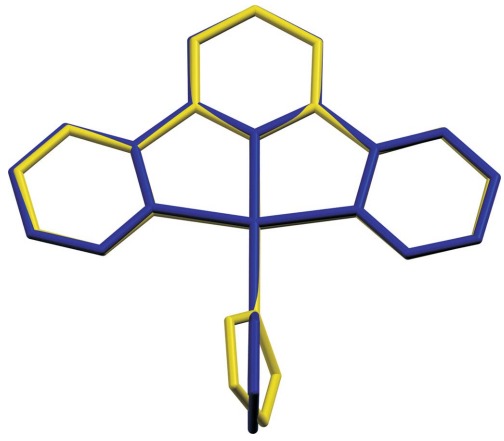

Figure 2
Least-squares fit of the non-H atoms of the DFT-calculated (dark; blue in the electronic version of the paper) and X-ray crystal structures (light; yellow) of $[Pt(pyz)(terpy)]^{2+}$, showing the similar coordination geometry of the platinum(II)–terpyridine unit and the difference in torsion angle of the pyrazole ligand.

The geometry-optimized cation shows that *in vacuo* the pyrazole ligand in the lowest-energy conformation is perpendicular to the terpyridine ligand (*i.e.* 90°). This conformation would lead to minimal nonbonded repulsion between the pyridine H atoms and the pyrazole ligand and as such is a low-energy structure. This orientation would also allow for π interaction between the pyrazole ligand and the d_{xy} orbital of the Pt^{II} atom, which is nonbonding with respect to the terpyridine ligand. In the solid-state structure, the pyrazole ligand is orientated at an angle of 62.4 (6)° relative to the terpyridine ligand. This deviation from the lowest-energy conformation is seemingly due to hydrogen bonding between the pyrazole NH group and the perchlorate anion in the lattice. It would appear that the stability gained through the hydrogen bonding is sufficient for the molecule to adopt a higher-energy conformation.

Aside from the torsion angle of the pyrazole ligand the calculated and experimental structures are very similar, with minimal differences in geometry about the Pt^{II} centre and the terpyridine ligand. The Pt—N bond lengths of the calculated and experimental structures are essentially equivalent (within 3σ); these bond lengths are summarized in Table 2. An overlay of the two structures has been calculated using *Mercury* 2.3 (Fig. 2) and shows that the solid-state structure deviates only slightly from the calculated lowest-energy conformation. This minimal deviation is indicated by the relatively small r.m.s. deviation of 0.202 Å.

Experimental

Chlorido(2,2′:6′,2″-terpyridine)platinum(II) chloride dihydrate, [Pt-Cl(terpy)]Cl·2H_2O, was synthesized as described by Pitteri *et al.* (1995). $AgClO_4$ (54 mg, 0.26 mmol) was added to [PtCl(terpy)]-Cl·2H_2O (70 mg, 0.13 mmol) dissolved in nitromethane (4 ml) and the resulting solution stirred at approximately 323 K for 1 h. The solution turned pale yellow and a white precipitate, AgCl(*s*), formed and was filtered off. Pyrazole (9 mg, 0.13 mmol) was added to the solution which immediately turned dark yellow in colour. Yellow crystals (yield 69%) were grown *via* vapour diffusion of diethyl ether into a concentrated solution of (I) in nitromethane.

Crystal data

$[Pt(C_3H_4N_2)(C_{15}H_{11}N_3)](ClO_4)_2\cdot CH_3NO_2$
M_r = 756.38
Monoclinic, $P2_1/c$
a = 16.351 (5) Å
b = 11.534 (4) Å
c = 14.075 (5) Å
β = 111.311 (5)°
V = 2472.9 (14) Å^3
Z = 4
Mo $K\alpha$ radiation
μ = 5.96 mm^{-1}
T = 296 K
0.60 × 0.40 × 0.20 mm

Data collection

Oxford Diffraction Xcalibur2 CCD diffractometer
Absorption correction: multi-scan (Blessing, 1995) T_{min} = 0.124, T_{max} = 0.382
16387 measured reflections
4877 independent reflections
3848 reflections with $I > 2\sigma(I)$
R_{int} = 0.057

Refinement

$R[F^2 > 2\sigma(F^2)]$ = 0.047
$wR(F^2)$ = 0.131
S = 1.02
4877 reflections
339 parameters
49 restraints
H-atom parameters constrained
$\Delta\rho_{max}$ = 2.24 e Å^{-3}
$\Delta\rho_{min}$ = −1.68 e Å^{-3}

The positions of all H atoms were calculated using the standard riding model of *SHELXL97*, with aromatic C—H = 0.93 Å and U_{iso}(H) = 1.2U_{eq}(C). The only exception was the pyrazole NH-group H atom which was located in a difference Fourier map and allowed to refine isotropically. The perchlorate O atoms were treated with a static disorder model with isotropic O atoms. This method led to a narrower range of Cl—O bond lengths and improved s.u. values when compared to a dynamic model. Each perchlorate anion shows orientational disorder. Around Cl1 there are two sets of possible positions defined by O1*A*/O2*A*/O3*A*/O4*A* and O1*B*/O2*B*/O3*B*/O4*B*, while around Cl2 the possible positions are O5*A*/O6*A*/O7*A*/O8*A* and O5*B*/O6*B*/O7*B*/O8*B*. The Cl—O distances were restrained to 1.43 (2) Å. The occupancies for sites *A* and *B* around Cl1 converged to 52.1 (5) and 47.9 (5)%, respectively, while around Cl2 the occupancies converged to 63.2 (5) and 36.8 (5)%, respectively.

Data collection: *CrysAlis CCD* (Oxford Diffraction, 2008); cell refinement: *CrysAlis CCD*; data reduction: *CrysAlis RED* (Oxford Diffraction, 2008); program(s) used to solve structure: *SHELXS97* (Sheldrick, 2008); program(s) used to refine structure: *SHELXL97* (Sheldrick, 2008); molecular graphics: *WinGX* (Farrugia, 1999); software used to prepare material for publication: *WinGX* and *publCIF* (Westrip, 2010).

Table 1
Hydrogen-bond geometry (Å, °).

D—H···*A*	*D*—H	H···*A*	*D*···*A*	*D*—H···*A*
N5—H5···O2*A*^{i}	0.86	2.16	2.85 (2)	134 (1)
C1—H1···O3*A*	0.93	2.47	3.31 (2)	149 (1)
C1*S*—H1*S*2···O1*A*	0.96	2.58	3.20 (2)	123 (1)
C1*S*—H1*S*3···O4*A*^{i}	0.96	2.46	3.40 (2)	170 (1)
C7—H7···O6*A*^{ii}	0.93	2.52	3.36 (2)	150 (1)
C8—H8···O8*A*^{i}	0.93	2.47	3.31 (2)	150 (1)
C14—H14···O8*A*^{iii}	0.93	2.41	3.08 (2)	128 (1)
C16—H16···O2*A*^{iv}	0.93	2.52	3.28 (2)	139 (1)

Symmetry codes: (i) $x, -y+\frac{1}{2}, z-\frac{1}{2}$; (ii) $x, y-1, z$; (iii) $x, -y+\frac{3}{2}, z-\frac{1}{2}$; (iv) $-x+1, y+\frac{1}{2}, -z+\frac{1}{2}$.

Table 2
Comparison of experimental and DFT-calculated bond lengths and angles (Å, °).

Bond/angle	Experimental length/angle	Calculated length/angle
Pt—N1	2.025 (7)	2.037
Pt—N2	1.924 (7)	1.954
Pt—N3	2.016 (7)	2.037
Pt—N4	2.012 (7)	2.035
N1—Pt—N2	80.9 (3)	81.1
N2—Pt—N3	81.5 (3)	81.1
N3—Pt—N4	99.4 (3)	98.89
N4—Pt—N1	98.2 (3)	98.89

We thank the University of KwaZulu–Natal and the National Research Foundation for their financial support.

Supplementary data for this paper are available from the IUCr electronic archives (Reference: OV3005). Services for accessing these data are described at the back of the journal.

References

Allen, F. H. (2002). *Acta Cryst.* B**58**, 380–388.
Bailey, J. A. & Gray, H. B. (1992). *Acta Cryst.* C**48**, 1420–1422.
Blessing, R. H. (1995). *Acta Cryst.* A**51**, 33–38.
Farrugia, L. J. (1999). *J. Appl. Cryst.* **32**, 837–838.
Field, J. S., Büchner, R., Haines, R. J., Ledwaba, P. W., Mcguire, R., McMillan, D. R. & Munro, O. Q. (2007). *Inorg. Chim. Acta*, **360**, 1633–1638.
Field, J. S., Haines, R. J. & Summerton, G. C. (2003). *J. Coord. Chem.* **56**, 1149–1159.
Frisch, M. J., *et al.* (2004). *GAUSSIAN03*. Revision C.02. Gaussian Inc., Wallingford, CT, USA.
Hay, P. J. & Dunning, T. H. Jr (1976). *Modern Theoretical Chemistry*, Vol. 3, pp. 1–28. New York: Plenum.
Hay, P. J. & Wadt, W. R. (1985*a*). *J. Chem. Phys.* **82**, 270–283.
Hay, P. J. & Wadt, W. R. (1985*b*). *J. Chem. Phys.* **82**, 284–298.
Hay, P. J. & Wadt, W. R. (1985*c*). *J. Chem. Phys.* **82**, 299–310.
Jaganyi, D., De Boer, K.-L., Gertenbach, J. & Perils, J. (2008). *Int. J. Chem. Kinet.* **40**, 808–818.
Oxford Diffraction (2008). *CrysAlis CCD* and *CrysAlis RED*. Versions 1.171.32.24. Oxford Diffraction Ltd, Yarnton, Oxfordshire, England.
Perdew, J. P., Burke, K. & Enzerhof, M. (1997). *Phys. Rev. Lett.* **78**, 1396.
Pitteri, B., Annibale, G. & Brandolisio, M. (1995). *Polyhedron*, **14**, 451–453.
Sheldrick, G. M. (2008). *Acta Cryst.* A**64**, 112–122.
Thurston, D. E. (2007). *Chemistry and Pharmacology of Anticancer Drugs*. Boca Raton: CRC Press Taylor and Francis Group.
Westrip, S. P. (2010). *J. Appl. Cryst.* **43**, 920–925.